Research Article

Journal of Environmental Nanotechnology

Metal–Organic Frameworks (MOFs) for Sustainable Water Disinfection: Synthesis, Characterization, and Antimicrobial Properties

Suman Thakur and Sharda Bharti*

Department of Biotechnology, National Institute of Technology (NIT) Raipur, Raipur, CG, India

Received: 04.05.2024 Accepted: 19.06.2024 Published: 30.06.2024

*sbharti.bt@nitrr.ac.in

ABSTRACT

Waterborne biological pollution poses a significant threat to both the environment and human health, leading to the transmission of various waterborne diseases. Ensuring the safety of drinking water is essential for safeguarding public health and reducing the prevalence of waterborne illnesses caused by microbial pollutants. Recently, there has been a notable increase in the utilization of nanoparticles for water treatment purposes. Metal-Organic Frameworks (MOFs) are emerging as promising candidates for enhancing water treatment processes due to their structural and functional adjustability and makes them stand out for environmental remediation. Notable properties include porous structures with customizable sizes, large surface areas, and internal characteristics that are variable. In this study, zeolitic-imidazolate frameworks (ZIF-8) and Ag@zeolitic-imidazolate frameworks (Ag@ZIF-8) were synthesized using 2-methylimidazole (2-MIM) as an organic linker via a facile green synthesis method and used for water disinfection. These MOFs were characterized using a range of techniques including UV-vis spectroscopy, FTIR, and X-ray diffraction, SEM/EDS. The antibacterial activity of ZIF-8 and Ag@ZIF-8 were evaluated using the disc diffusion method against Gram-negative and Gram-positive bacteria, i.e., *E. coli* and *S. aureus*, respectively. These MOFs demonstrated strong antimicrobial activity against both Gram-positive *S. aureus* and Gram-negative bacteria *E. coli*, where the Ag-ZIF-8 MOF exhibited improved antibacterial activities over ZIF-8 alone. Finally, the suggested material shows promise for reusable water filtration and disinfection against a variety of pollutants, providing a practical option to reduce environmental and public health threats.

Keywords: Antimicrobial properties; Environmental remediation; Metal-organic frameworks; Water disinfection; Zeolitic-imidazolate frameworks.

1. INTRODUCTION

Waterborne biological pollution is a serious hazard to both the environment and human health since it may cause the spread of a variety of waterborne illnesses. Biological contamination of drinking water refers to microorganisms such as bacteria, viruses, fungi, protozoa, and helminths in water sources suitable for human use (Kumar *et al.* 2022). Metal-organic frameworks (MOFs) might be employed as antibacterial agents as well as water treatment materials. Metal ions or clusters interact with organic ligands to form MOFs. Over the last two decades, there have been significant advances in MOF research in the field of solid-state chemistry (Amargeetha *et al.* 2018). Metal-organic frameworks (MOFs) are particularly desired porous materials due to their outstanding features, such as a surprisingly high specific surface area, extraordinary thermal and chemical durability across a broad variety of situations, and the flexibility to modify pore sizes (Thakur *et al.* 2023). The extensive use of MOFs in many industries is attributed to their exceptional advantages. Recent researchers have indicated that MOFs are highly regarded as potential supports for metal nanoparticles and are considered to be superior to other porous materials such as clay, zeolites, and silica in a wide range of applications (Gu *et al.* 2020). Zeolitic imidazolate frameworks, often known as ZIFs, have shown substantial development in recent years. The structures of these compounds are based on tetrahedral units, where each metal ion (M) (such as Zn or Co) is bound to four organic imidazolate (Im) linkers (M−Im−M). Zeolitic Imidazolate Frameworks (ZIFs) are considered a subset of Metal-Organic Frameworks (MOFs), and traditionally, their structure has closely matched that of zeolites (Shahsavari *et al.* 2022). ZIFs possess the desirable attributes of both MOFs and zeolites, such as porosity, crystallinity, and remarkable chemical and thermal stability. Regarding its diameter and pore width, it has a value of 3.4 Å and 11.6 Å, respectively. The structure of ZIF-8 ($Zn(mIm)_2$), in which mIm is the 2-methyl imidazolate, is characterized by a solidate/sodalite (SOD) architecture, and it possesses a space group consisting of linked six-membered ring windows (Bergaoui *et al.* 2021). ZIF-8 is the most well-known and established member of the ZIF family, and as

a result, a significant amount of research is being conducted on the unique characteristics and uses of the ZIF family. Furthermore, ZIFs are considered attractive choices for several purposes such as sensing, catalysis, adsorption, membrane gas separation, and antimicrobial applications (Salehipour *et al.* 2021). One of the advantages of ZIF-8 nanoparticles is that their extraordinary stability makes it possible for them to be used for extended periods of time (Yuan *et al.* 2017).

MOF is a suitable material for incorporating silver nanoparticles (AgNPs), and the presence of Zn^{2+} cations in the ZIF-8 structure enhances the antibacterial activity of silver ions through a synergistic effect (Abdi, 2020). Silver nanoparticles have attracted significant attention for their potential as antimicrobial agents in combating bacterial infections. Due to their distinctive characteristics, such as a high ratio of surface area to volume and potent antibacterial capabilities, they are considered very promising for a range of applications, including antimicrobial (Bharti *et al.* 2019; Bharti *et al.* 2020; Bharti *et al.* 2021) and biomedical/therapeutic applications (Bharti *et al.* 2023b; Bharti *et al.* 2023a; Bharti *et al.* 2024). This antimicrobial action is achieved by disrupting the cell membrane, entering the microorganism, and harming the cell. It was discovered that AgNPs had a significantly lower effect on the Gram-positive bacteria because of the structural difference in the composition of the cell walls between Gram-positive and Gram-negative bacteria. Gram-negative bacteria possess an outer coating of lipopolysaccharides, which is situated beneath a thin layer of peptidoglycan measuring 7-8 nm in thickness. In contrast, the cell wall of Gram-positive bacteria mostly consists of a substantial layer (20–80 nm) of peptidoglycan. This peptidoglycan is made up of linear polysaccharidic chains that are crosslinked by short peptides, resulting in a solid three-dimensional structure. The rigidity and the widespread formation of chemical bonds not only decrease the locations on the bacterial cell wall where AgNPs may attach, but also make it more challenging for the particles to enter the wall (Franci *et al.* 2015). The incorporation of MOFs with inorganic compounds can significantly enhance the antibacterial efficacy of the complexes. The bacterial inhibitory activity was improved by combining ZIF-8 with Ag in this experiment. ZIF-8, due to the presence of the Zn^{2+} core metal ion, has antibacterial properties and can be utilized as an antibacterial agent (Bao *et al.* 2023). Guo et al. effectively produced core-shell Ag@ZIF-8 nanowires, which exhibited notable antibacterial properties against *E. coli* and B. subtilis (Guo *et al.* 2018). Malik and colleagues produced multifunctional CdSNPs@ZIF-8 nanoparticles that exhibit antibacterial properties against both *E. coli* and *S. aureus* (Malik *et al.* 2018).

In this work, for this investigation, we utilized a straightforward and eco-friendly green synthesis technique to accomplish the fabrication of ZIF-8 and Ag@ZIF-8. Various analytical methods, including UV-Vis spectrophotometry, Fourier-transform infrared spectroscopy (FT-IR), X-ray diffraction (XRD), and scanning electron microscopy combined with energy-dispersive X-ray spectroscopy (SEM/EDS), were used to completely characterize the resulting nanomaterials. The antibacterial activity of the synthesized materials was then tested using the zone of inhibition test against both Gram-positive (*S. aureus*) and Gram-negative (*E. coli*) bacteria. The MOF: ZIF-8 and Ag@ZIF-8 (Ag-MOF) nanocomposites both were subjected to this examination to examine the antibacterial properties. Overall, this research shows potential for creating new antimicrobial materials that might be used in several areas such as medicine, biotechnology, and environmental remediation. More investigation in this area may help find solutions to the problems caused by antibiotic resistance and bacterial infections.

2. MATERIALS AND METHODS

2.1 Materials

The used chemicals and reagents include- zinc nitrate hexahydrate ($Zn(NO_3)_2$•$6H_2O$, ≥99.0%), silver nitrate ($AgNO_3$, ≥99.8%) were acquired from Merck, 2-methylimidazole (Hmim, ≥99.0%), cobalt nitrate hexahydrate ($Co(NO_3)_2$•$6H_2O$, ≥99.0%) were purchased from LOBA CHEM, India. Nutrient broth and bacteriological nutrient agar were purchased from HiMedia, India. Other chemicals i.e., ethanol, NaOH, HCl were of analytical grade, which were used as received. All chemicals in this research were used directly without any additional purification. Furthermore, the antibacterial efficacy of the MOF and Ag-MOF were assessed using two bacterial strains, a Gram-negative bacterium, Escherichia coli and a Gram-positive bacterium, Staphylococcus aureus (MTCC 9542), which were obtained from Institute of Microbial Technology (IMTECH, Chandigarh), India.

2.2 Methods

2.2.1 Synthesis of ZIF-8

ZIF-8 was synthesised in this work according to Abdi with slight modification (Abdi, 2020). Fig. 1 illustrates the synthesis process of ZIF-8 nanoparticles. To prepare ZIF-8, a precursor solution comprising zinc cations ($Zn(NO_3)_2$·$6H_2O$), H-MIM (2-methylimidazole) ligand, and deionized water was utilized. Initially, 1.487 g of $Zn(NO3)_2$·$6H_2O$ (0.05 M) was dissolved in deionized water. Simultaneously, 12.317 g of H-MIM (1.5 M) was dissolved in deionized water separately. The solution containing zinc nitrate was then slowly added dropwise to the solution containing the organic ligand. The resulting mixture was stirred using a magnetic stirrer for 2 hours at room temperature, maintaining a speed of 300 rpm, and adjusting the pH to 8. Subsequently, the

milky white solution was centrifuged to separate the ZIF-8 particles. These particles were washed multiple times with ethanol and then with deionized water. Finally, the particles were dried overnight at 50˚C.

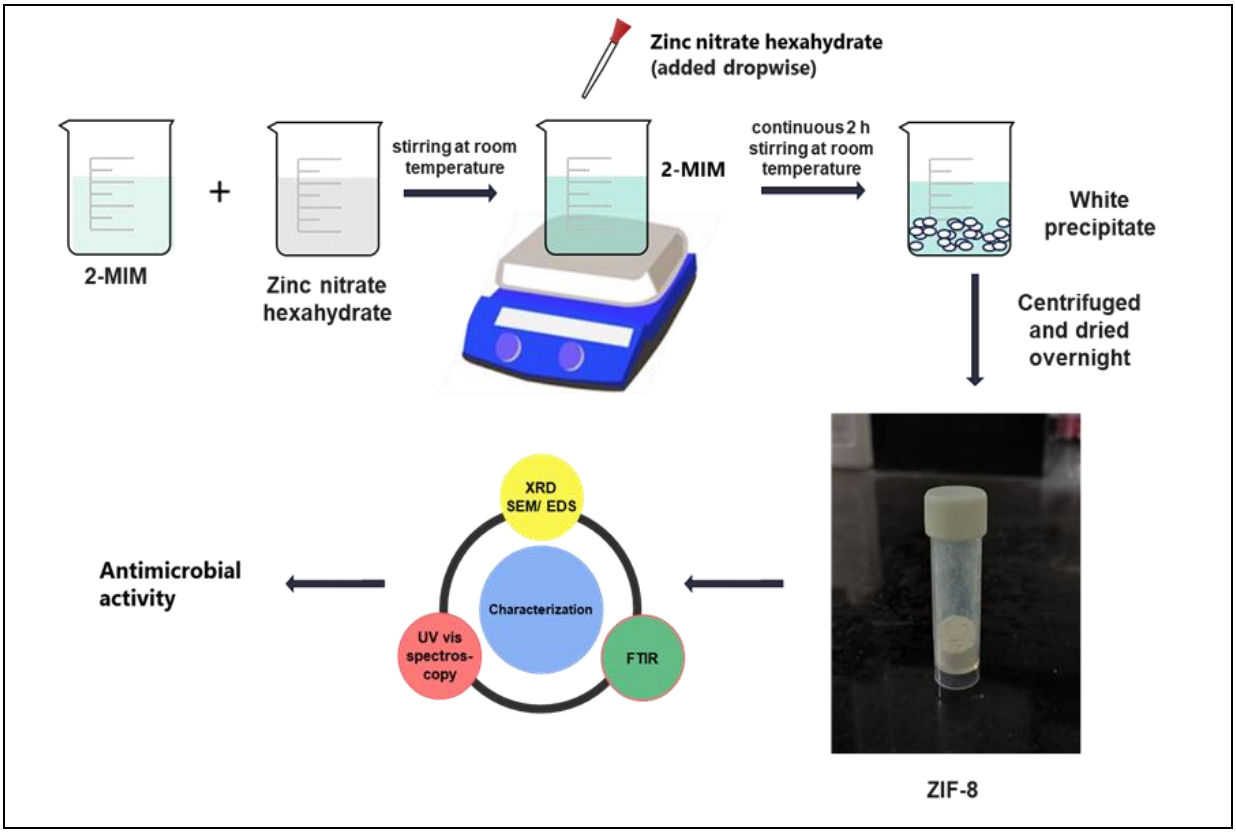

Fig. 1: Schematic representation of synthesis of ZIF-8

2.2.2 Synthesis of Ag@ZIF-8

The synthesis of Ag@ZIF-8 was conducted following the method described by Abdi (2020) with minor modifications. Initially, 0.125 grams of $AgNO_3$ were introduced into a solution consisting of 20 mL of ethanol and deionized water. The resulting mixture was then agitated using a magnetic stirrer for 30 minutes at a speed of 300 revolutions per minute, all at room temperature. Subsequently, 0.5 gram of the synthesized ZIF-8 powder were evenly distributed throughout the mixture and stirred for two hours. The sample has been designated as Ag@ZIF-8 nanocomposites. Subsequently, the Ag@ZIF-8 samples were separated using centrifugation, subjected to three rounds of ethanol washing to eliminate any remaining Ag^+ ions adsorbed onto the ZIF-8 MOF particles, and then dried at a temperature of 50 °C in an oven. The dried Ag@ZIF-8 nanocomposites were used for characterization and to assess their antimicrobial properties.

2.3 Characterization

The functional groups were characterised by detecting the molecular vibrations of the materials using Fourier transforms infrared spectra (Alpha II, Bruker). The materials were compressed into pellets, and the 500–4500 cm^{-1} IR absorption range was recorded. UV-Vis spectra was recorded using Double beam UV-vis spectroscopy (1900i, Toshvin Analytical) in the range between 200–900 nm for the synthesized nanomaterials. The broad angle X-ray diffraction of the ZIF-8 and Ag@ZIF-8 nanocomposites was measured throughout a scanning range of 10° to 80° using X-ray diffractometer (PANalytical 3 kW X'pert Powder XRD – Multifunctional). The SEM (Scanning Electron Microscopy) used to examine the surface morphologies of the material using ZEISS EVO Series Scanning Electron Microscope EVO 18.

2.4 Disc Diffusion Studies for Depicting Antibacterial Activity

The experiment utilised a newly obtained culture of Gram-positive *S. aureus* MTCC 9542 and Gram-negative *E. coli* K-12. Initially, all glassware and samples were subjected to sterilisation by placing them in an autoclave at a temperature of 120 °C for a duration of 30 minutes. Both strains were added into a flask containing 100 ml of nutrient broth separately and cultivated for 24 hours in a rotary shaker incubator at 120 revolutions per minute. Subsequently, the nutritional agar culture medium was sterilized and added to the

individual sterile petri plates. The antibacterial properties of ZIF-8 and Ag@ZIF-8 were assessed using zone inhibition tests. This involved using loaded discs (60 µL of 20 mg/mL) of the material with a pore size of 0.2 µm and a diameter of 1 cm, as described by Bharti *et al.* 2021. Prior to the placement of the discs, a 100 µL bacterial solution with a concentration of 104 CFU/ml was uniformly distributed over nutritional agar plates. Following placement on individual plates, the discs loaded with MOF and Ag-MOF nanocomposites (NP-laden discs) and the control disc (which did not contain any nanoparticles) were subjected to a 24-hour incubation period at a temperature of 37 °C. After 24 hours of incubation, the zone of inhibition (ZOI) was measured for each bacterial strain using a ruler. The results were reported as the mean value of ZOI (mm) ± the standard deviation (SD), which were calculated from three repeated measurements.

3. RESULT AND DISCUSSION

3.1 Synthesis and Characterization

The ZIF-8 and Ag@ZIF-8 materials were successfully synthesised using a simple and environmentally friendly synthesis process. The precursor salts employed were zinc nitrate hexahydrate ($Zn(NO3)_2{\cdot}6H_2O$) and silver nitrate ($AgNO_3$). The organic ligand employed was H-MIM, while the solvent consisted of a mixture of ethanol and deionized water. Due to its predominant interaction with metal ions, alcohol played a crucial role in the initiation of ZIF formation and the subsequent growth of crystals resulting from the combination of metal and ligand solutions. Water or ethanol are used as solvents to aid in the creation of a mixture and the dissolving of reactants, which is essential to produce ZIF crystals of superior quality. The other synthesis parameters, such as temperature, pH, stirring power, and reaction time, were kept constant. Following the synthesis, the material was washed using centrifugation. The resulting pellets were then resuspended in ethanol and subsequently in deionized water for further washing. These samples were then employed for characterization and antibacterial investigations. The materials were characterized using UV-vis spectroscopy to determine their optical properties, FTIR to identify molecular vibrations, XRD to assess the phase development and purity of the synthesized MOFs, and SEM/EDS to analyze the morphology and validate the existence of components in the material.

3.1.1 UV-vis Spectroscopy

As shown in Fig.2, ultraviolet-visible (UV-Vis) spectra of ZIF-8 samples were recorded from 200 to 800 nm. The ZIF and AgNO@ZIF-8 samples exhibited identical UV-Vis spectra. ZIF-8 showed a maximum absorption peak at 217 nm. Before taking the absorbance sonication was done for few minutes for both the samples because ZIF-8 is insoluble in water. In Ag@ZIF-8 absorption peak, some changes were observed due to the presence of Ag in ZIF-8.

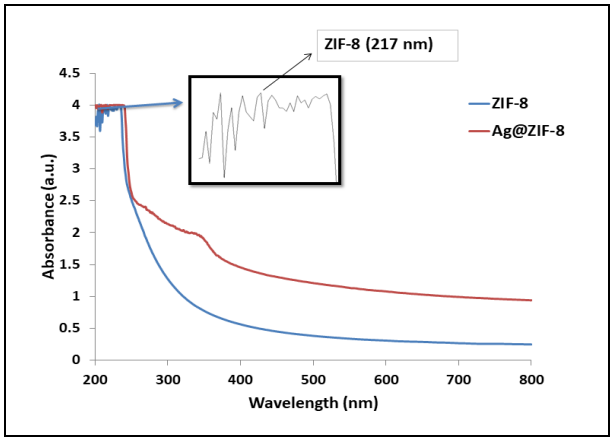

Fig. 2: UV-vis spectra of ZIF-8 and Ag@ZIF-8

3.1.2 XRD Analysis

The crystallinity of the pure ZIF-8 and Ag@ZIF-8 structures was assessed using XRD analysis. The synthesised ZIF-8 pattern (Fig. 3) is consistent with earlier research reported in literature sources (Abdi, 2020; Subhadarshini *et al.* 2023). The clearly visible and strong peaks seen at different 2θ values, as shown in Table 1, indicate that ZIF-8 has a sodalite (SOD)-type structure with excellent crystallinity (Shahsavari *et al.* 2022). The presence of a strong diffraction peak (011) at an angle of 7.2° shows that ZIF-8 has a highly crystalline structure (Du *et al.* 2021). In addition, the diffraction peaks of silver with a face-centered cubic structure may be clearly observed at 2θ = 38° and 44.2° for the (111) and (200) planes, respectively, as reported by Meng *et al.* 2020. Significantly, the introduction of Ag results in a reduction in the intensity of distinct diffraction peaks, indicating the effective integration of Ag ions into the porous structure and surface of ZIF-8.

Table 1. Summary of 2θ value of XRD spectra of ZIF-8 and Ag@ZIF-8 and their corresponding lattice plane

2θ value	Plane	2θ value	Plane
7.29°	011	18.03°	222
10.34°	002	22.12°	114
12.70°	112	24.49°	233
14.67°	022	26.65°	134
16.45°	013		

3.1.3 FTIR analysis

The FTIR analysis was conducted across a range of wavenumbers from 3500 to 600 cm^{-1} to determine the specific bonding groups present in the synthesized MOFs. The prominent bands of the ZIF-8

crystal are linked to the organic ligand H-MIM in the infrared spectrum, as seen in Fig. 4 and outlined in Table 2.

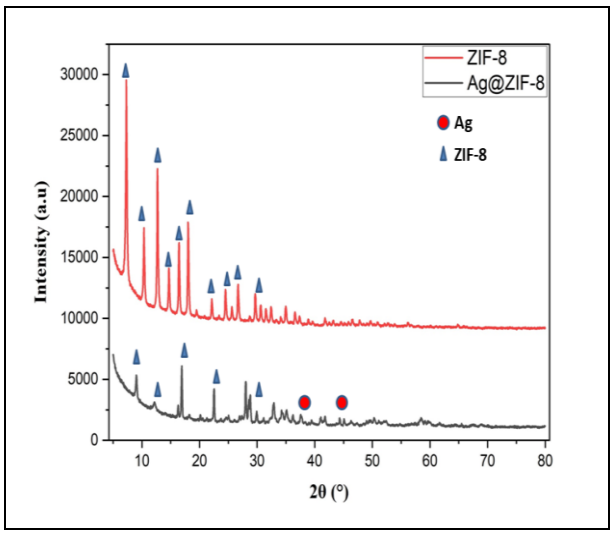

Fig. 3: XRD patterns of ZIF-8 and Ag@ZIF-8

Table 2. FTIR spectra depicting presence of various functional groups of ZIF-8

Frequency range (cm^{-1})	Functional group
1573	C-N (H-MIM)
2920	C-H bond stretching mode of H-MIM
1428	Stretching vibration of H-MIM
1629	O-H bending vibration
600-1350 and 1350-1500	Bending and stretching vibrations of H-MIM
1144 and 1307	H-MIM bending signals

The characteristic peaks between 600 and 1500 cm^{-1} wavenumbers may be linked to the bending and stretching modes of imidazole rings. Specifically, the range of 600-1350 cm^{-1} corresponds to the bending mode of H-MIM, while the range of 1350-1500 cm^{-1} corresponds to the stretching mode of H-MIM (Abdi, 2020). The distinctive peak at 1428 cm^{-1} reveals the stretching vibration of the imidazole ring (Rahmati et al., 2020). The absorption band at 1573 cm^{-1} is attributed to the stretching vibration of the C=N bond, whilst the peaks at 1144 cm^{-1} and 1307 cm^{-1} correspond to the bending signals of the imidazole ring (Rahmati *et al.* 2020).

The peaks seen at 993 cm^{-1} and 752 cm^{-1} can be ascribed to the bending vibrations of the C-N and C-H bonds, respectively. The O-H bending vibration band is found at 1629 cm^{-1} (Abdi, 2020).

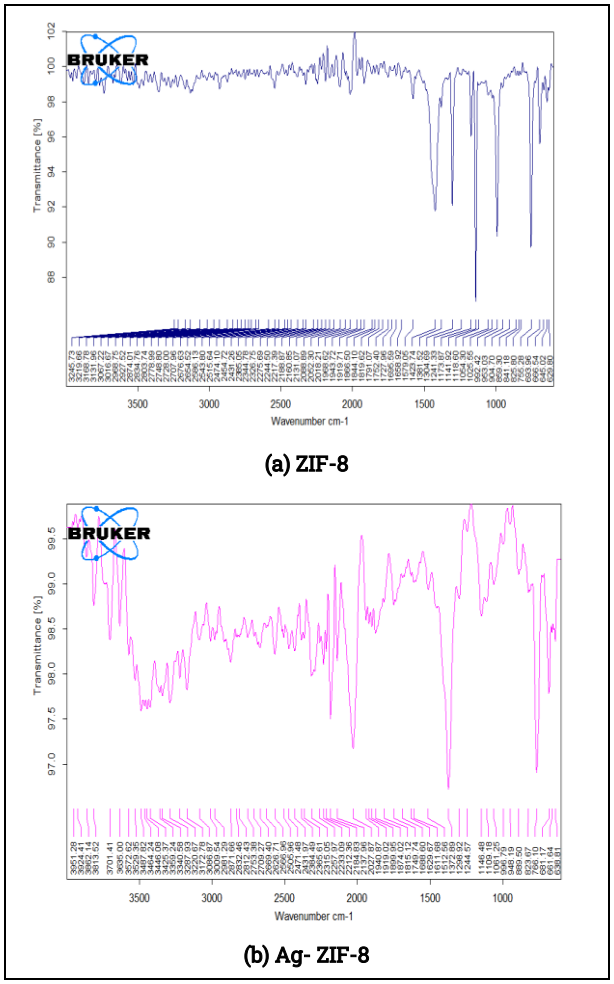

Fig. 4: FTIR spectra of the prepared samples a) ZIF-8 b) Ag@ZIF-8

3.1.4 Morphological Analysis

The morphology of the synthesised materials was studied in SEM as shown in Fig. 5. ZIF-8 particles exemplify non-uniform size because of several conditions on the nucleation process and crystal formation. The rough surface of Ag@ZIF-8, as seen in Fig. 5, is a result of the Ag particles being attached to the surface of the ZIF-8 material. Tiny white circles Fig. 5 (b, d, f) provides evidence of the existence of Ag. Additional confirmation of the Ag, Zn, C, and O components in ZIF-8 and Ag@ZIF-8 is provided by the elemental studies performed using EDS. The atomic % and weight % of all the elements (Ag, Zn, C, O) are presented in Fig.6 (b and d).

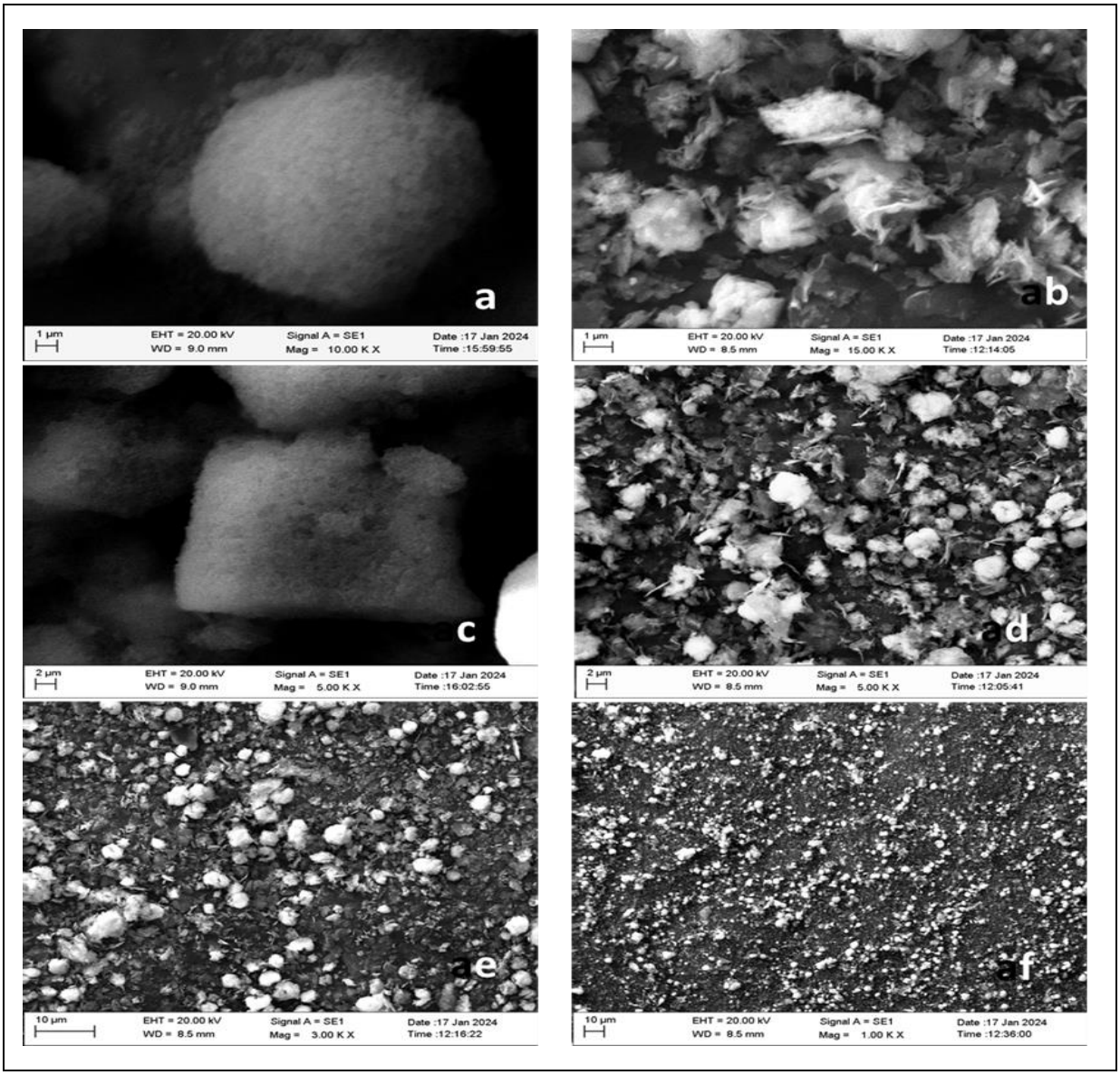

Fig. 5: SEM images of (a,c,e) ZIF-8; (b,d,f) Ag@ZIF-8

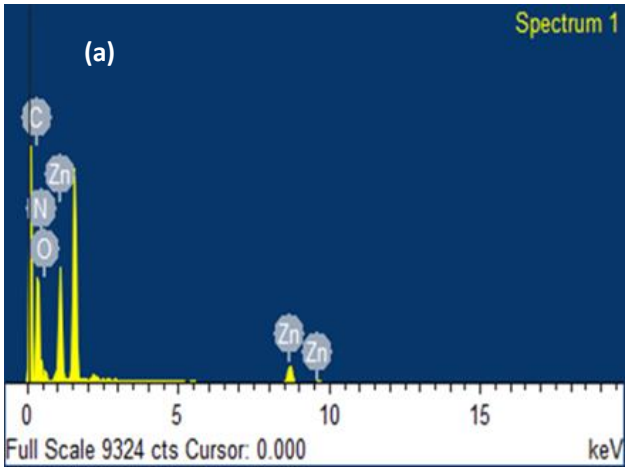

(b)

Element	Weight%	Atomic%
C K	11.57	20.16
O K	53.76	70.36
Zn K	21.81	6.98
Ag L	12.86	2.50
Totals	100.00	

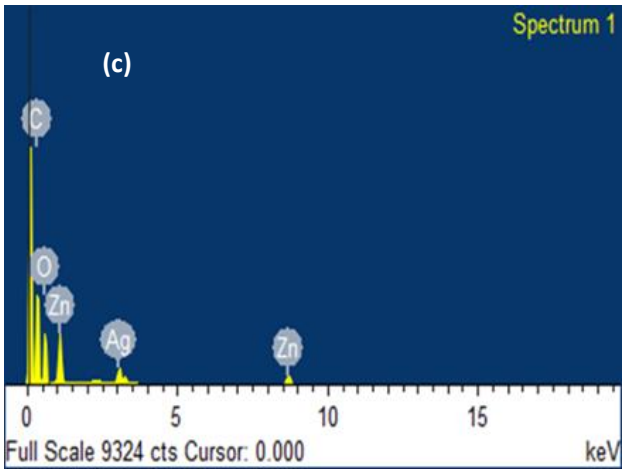

(d)

Element	Weight%	Atomic%
C K	11.57	20.16
O K	53.76	70.36
Zn K	21.81	6.98
Ag L	12.86	2.50
Totals	100.00	

Fig. 6: EDS elemental analysis of the ZIF-8 (a and b) and Ag@ZIF-8 (c and d)

Fig. 7: Inhibition zone of ZIF-8 and Ag@ZIF-8 against *E. coli* and *S. aureus*

Table 3. Displays a previous study on antibacterial activity using Ag/ZIF-8 composite

Sample	Zone of inhibition (mm)		Reference
	E. coli	*S. aureus*	
Ag@ZIF-8	ZIF-8 = 10 mm; Ag@ZIF-8 = 23 mm	ZIF-8 = 14.8 mm; Ag@ZIF-8 = 25.2 mm	Abdi, 2020
Ag@ZIF-8	ZIF-8 = no zone; Ag@ZIF-8 = 13 mm	ZIF-8 = no zone Ag@ZIF-8 = 18 mm	Subhadarshini et al., 2023
AgTiO2/ZIF-8	AgTiO2 = 17.6 mm; AgTiO2/ZIF-8 = 22.8 mm	-	Bao et al., 2023
ZIF-8/GO/ MgFe2O4/ TC	TC = 17 mm ZIF-8/GO/ MgFe2O4 = no zone; ZIF-8/GO/ MgFe2O4/TC = 22 mm	TC = 18 mm ZIF-8/GO/MgFe2O4 = no zone; ZIF-8/GO/ MgFe2O4/TC = 25 mm	Sanaei-Rad et al., 2021
Ag@ZIF-8	ZIF-8 = 11.5 mm Ag@ZIF-8 = 29.5 mm	ZIF-8 = 8 mm Ag@ZIF-8 = 21 mm	**This work**

3.2 Disc Diffusion Studies

The antibacterial activity of the synthesised substance was tested by ZOI assay. The inhibition zone diameters for pure ZIF-8 were obtained 11.5 mm and 8 mm for E.coli and *S. aureus*, respectively, while the inhibition zone diameter values for Ag@ZIF-8 were 29.5 mm and 21 mm for *E. coli* and *S. aureus*, respectively (Fig. 7). The results indicate that Ag doped ZIF-8 has excellent antibacterial properties against both Gram-positive and Gram-negative bacteria. In a separate investigation conducted by Subhadarshini *et al.* 2023, ZOI testing was conducted against *E. coli* and *S. aureus*. It was shown that pure ZIF-8 did not exhibit any ZOI against either strain.

However, Ag/ZIF-8 demonstrated ZOI with diameter values of 13 mm and 18 mm against *E. coli* and *S. aureus*, respectively (Subhadarshini *et al.* 2023). In their study conducted in 2020, Abdi et al. tested the antibacterial properties of Ag@ZIF-8 against two strains. The results showed that the zone of inhibition (ZOI) for pure ZIF-8 was 10 mm and 14.8 mm, respectively. In contrast, Ag@ZIF-8 exhibited ZOI values of 23 mm and 25.2 mm against *E. coli* and *S. aureus*, respectively. Clearly, the nanocomposite exhibited good antibacterial effectiveness compared to both the single pure ZIF-8 and AgNPs, as listed in Table 3.

3.3 Antibacterial Mechanism

Based on the experimental results, it is possible to conclude that Ag@ZIF-8 has superior antibacterial activity than ZIF-8 which is also reported by other researchers (Rahmati *et al.* 2020). The following was suggested as potential antibacterial mechanism of AgNPs, ZIF-8 and Ag@ZIF-8. Higher ZOI in case of Ag@ZIF-8 may be attributed to AgNPs and released silver ions causing inhibition of the bacterial growth of bacteria (Rahmati *et al.* 2020). Various mechanisms have been documented that pertain to the antibacterial agent role of AgNPs, as illustrated in Fig. 8. Due to affinity for sulphur-containing proteins of Ag, which can damage or alter the structures of strains, AgNPs can adhere to the cell membranes of bacteria (Thakur *et al.* 2023). By complexing with RNA and DNA, AgNPs can condense and prevent DNA replication. This binding of AgNPs with thiol groups in proteins deactivates the function of respiratory enzymes. Released a free radical on the exterior AgNPs exhibit antibacterial properties (Bharti *et al.* 2021). Furthermore, the interactions between Ag^+ and structure of DNA can inhibit bacterial growth. As a result, the bacteria cell growth is inhibited, cell membrane gets ruptured leading to cell death as the outer layer loses their protection. AgNPs cause oxidative stress cells by producing reactive oxygen species (ROS), damage proteins and nucleic acids, and ultimately stop cells from proliferating (Bharti *et al.* 2020; Bharti *et al.* 2023a). Furthermore, when Ag@ZIF-8 is added to bacterial solution, it can release Zn^{2+} and Ag^+ with less toxicity and biological antibacterial activity, these metal ions come into close contact with bacteria, they can attach themselves to the component proteins in their cell walls and membranes, denaturing and deactivating them (Cao *et al.* 2020; Yan *et al.* 2022). The inherent antibacterial characteristic of metal ions liberated from zinc ions is thought to be the cause of antimicrobial effect of ZIF-8. Because ZIF-8 has a porous structure and a high BET surface area, more Ag is equally spread on its surface. This increases the area of contact between the bacteria and the bactericidal agent, enhancing the antibacterial activity. Furthermore, Ag@ZIF-8 can be gradually released to release Ag^+ and Zn^{2+}, which would provide a sustained antibacterial action (Yan *et al.* 2022). In conclusion, Ag@ZIF-8 strong antibacterial activity results from their synergistic actions.

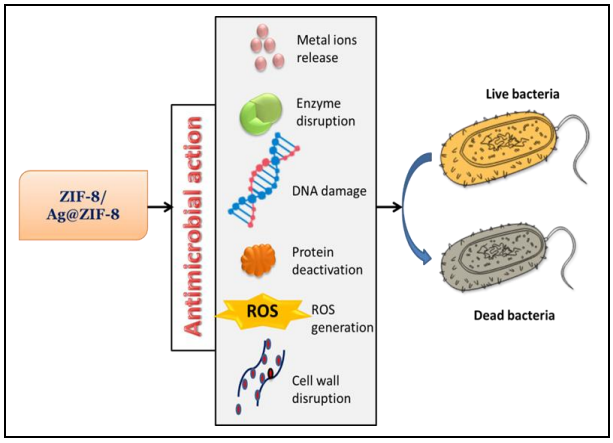

Fig. 8: Possible mode of antimicrobial action of ZIF-8/ Ag@ZIF-8

4. CONCLUSION

The MOFs, ZIF-8 and Ag@ZIF-8 were successfully produced employing a basic green synthesis process at room temperature. The effective synthesis of these materials was proven using various characterization techniques such as, UV-vis spectrophotometry, FTIR, XRD, and SEM/EDS. To examine the antibacterial activity of ZIF-8 and Ag@ZIF-8, we conducted zone of inhibition tests against Gram-positive (*S. aureus* MTCC 9542) and Gram-negative (*E. coli*) bacteria. Pure ZIF-8 suppressed the growth of *S. aureus* and *E. coli* with inhibition zone sizes of 11.5 mm and 8 mm, respectively. In comparison, Ag@ZIF-8 displayed inhibitory zone diameters of 29.5 mm and 21 mm for *S. aureus* and *E. coli*, respectively. The results suggest that Ag@ZIF-8 exhibits enhanced antibacterial efficacy compared to pure ZIF-8 against both pathogens. Our findings collectively highlight the promising potential of exploring silver nanoparticles, various ZIFs, and their synergistic effects as avenues for developing novel antimicrobial medicines. By further investigating these nanomaterials and their interactions, we can potentially unlock new strategies for combating bacterial infections and addressing the challenges of antimicrobial resistance with decreased adverse effects.

FUNDING

This research received no specific grant from any funding agency in the public, commercial, or not-for-profit sectors.

CONFLICTS OF INTEREST

The authors declare that there is no conflict of interest.

CREDIT AUTHOR STATEMENT

Suman Thakur: Writing- Conducted experiments, Data analysis, original draft preparation. Sharda Bharti: Conceptualization, Data analysis, Reviewing and Editing, Visualization, Supervision.

ACKNOWLEDGEMENTS

The authors would like to acknowledge the National Institute of Technology (NIT) Raipur for offering the necessary facilities to carry out this work, for partial funding support through Seed Grant Project (NITRR/Dean(R&C)/2022/85), and all other support in completing this manuscript.

COPYRIGHT

REFERENCES

Abdi, J., Synthesis of Ag-doped ZIF-8 photocatalyst with excellent performance for dye degradation and antibacterial activity, *Colloids Surfaces A Physicochem. Eng. Asp.* 604, 125330 (2020). https://doi.org/10.1016/j.colsurfa.2020.125330

Amargeetha, A., Velavan, S., X-ray Diffraction (XRD) and Energy Dispersive Spectroscopy (EDS) Analysis of Silver Nanoparticles Synthesized from Erythrina Indica Flowers, *Nanosci. Technol. Open Access* 5(1), 1–5 (2018). https://doi.org/10.15226/2374-8141/5/1/00152

Bao, S., Sun, S., Li, L., Xu, L., Synthesis and antibacterial activities of Ag-TiO2/ZIF-8, Front Bioeng Biotechnol. https://doi.org/10.3389/fbioe.2023.1221458

Bergaoui, M., Khalfaoui, M., Awadallah-F, A., Al-Muhtaseb, S., A review of the features and applications of ZIF-8 and its derivatives for separating CO2 and isomers of C3- and C4-hydrocarbons, *J. Nat. Gas Sci. Eng.* 96, 104289 (2021). https://doi.org/10.1016/j.jngse.2021.104289

Bharti, S., Anant, P. S., Kumar, A., Nanotechnology in stem cell research and therapy, *J. Nanoparticle Res.* 25(1), 6 (2023a). https://doi.org/10.1007/s11051-022-05654-6

Bharti, S., Kumar, A., Synergies in stem cell research: Integrating technologies, strategies, and bionanomaterial innovations, *Acta Histochem.* 126(1), 152119 (2024). https://doi.org/10.1016/j.acthis.2023.152119

Bharti, S., Mukherji, S., Mukherji, S., Extracellular synthesis of silver nanoparticles by Thiosphaera pantotropha and evaluation of their antibacterial and cytotoxic effects, *3 Biotech* 10(6), 237 (2020). https://doi.org/10.1007/s13205-020-02218-0

Bharti, S., Mukherji, S., Mukherji, S., Water disinfection using fixed bed reactors packed with silver nanoparticle immobilized glass capillary tubes, *Sci. Total Environ.* 689, 991–1000 (2019). https://doi.org/10.1016/j.scitotenv.2019.06.482

Bharti, S., Mukherji, S., Mukherji, S., Enhanced antibacterial activity of decahedral silver nanoparticles, *J. Nanoparticle Res.* 23(2), 36 (2021). https://doi.org/10.1007/s11051-020-05106-z

Bharti, S., Nag, P., Sadani, K., Mukherji, S., Mukherji, S., Exploring the Application, Safety, and Challenges of Free Versus Immobilized Antimicrobial Nanomaterials, In: Applications of Nanotechnology in Microbiology. Springer Nature Switzerland, Cham, pp 97–133 (2023). https://doi.org/10.1007/978-3-031-49933-3_5

Cao, P., Wu, X., Zhang, W., Zhao, L., Sun, W., Tang, Z., Killing Oral Bacteria Using Metal-Organic Frameworks, *Ind. Eng. Chem. Res.* 59(4), 1559–1567 (2020). https://doi.org/10.1021/acs.iecr.9b05659

Du, P. D., Hieu, N. T., Thien, T. V., Ultrasound-Assisted Rapid ZIF-8 Synthesis, Porous ZnO Preparation by Heating ZIF-8, and Their Photocatalytic Activity, *J. Nanomater.* 2021, 1–12 (2021). https://doi.org/10.1155/2021/9988998

Franci, G., Falanga, A., Galdiero, S., Palomba, L., Rai, M., Morelli, G., Galdiero, M., Silver Nanoparticles as Potential Antibacterial Agents, *Molecules* 20(5), 8856–8874 (2015). https://doi.org/10.3390/molecules20058856

Gu, A., Chen, J., Gao, Q., Khan, M. M., Wang, P., Jiao, Y., Zhang, Z., Liu, Y., Yang, Y., The preparation of Ag/ZIF-8@ZIF-67 core-shell composites as excellent catalyst for degradation of the nitroaromatic compounds, *Appl. Surf. Sci.* 516, 146160 (2020). https://doi.org/10.1016/j.apsusc.2020.146160

Guo, Y.-F., Fang, W.-J., Fu, J.-R., Wu, Y., Zheng, J., Gao, G.-Q., Chen, C., Yan, R.-W., Huang, S.-G., Wang, C.-C., Facile synthesis of Ag@ZIF-8 core-shell heterostructure nanowires for improved antibacterial activities, *Appl. Surf. Sci.* 435, 149–155 (2018). https://doi.org/10.1016/j.apsusc.2017.11.096

Kumar, P., Gacem, A., Ahmad, M. T., Yadav, V. K., Singh, S., Yadav, K. K., Alam, M. M., Dawane, V., Piplode, S., Maurya, P., Ahn, Y., Jeon, B. H., Cabral-Pinto, M. M. S., Environmental and human health implications of metal(loid)s: Source identification, contamination, toxicity, and sustainable clean-up technologies, *Front. Environ. Sci.* 10(August), 1–23 (2022). https://doi.org/10.3389/fenvs.2022.949581

Malik, A., Nath, M., Mohiyuddin, S., Packirisamy, G., Multifunctional CdSNPs@ZIF-8: Potential Antibacterial Agent against GFP-Expressing Escherichia coli and Staphylococcus aureus and Efficient Photocatalyst for Degradation of Methylene Blue, *ACS Omega* 3(7), 8288–8308 (2018). https://doi.org/10.1021/acsomega.8b00664

Meng, X., Duan, C., Zhang, Y., Lu, W., Wang, W., Ni, Y., Corncob-supported Ag NPs@ ZIF-8 nanohybrids as multifunction biosorbents for wastewater remediation: Robust adsorption, catalysis and antibacterial activity, *Compos. Sci. Technol.* 200, 108384 (2020). https://doi.org/10.1016/j.compscitech.2020.108384

Rahmati, Z., Abdi, J., Vossoughi, M., Alemzadeh, I., Ag-doped magnetic metal organic framework as a novel nanostructured material for highly efficient antibacterial activity, *Environ. Res.* 188, 109555 (2020). https://doi.org/10.1016/j.envres.2020.109555

Salehipour, M., Rezaei, S., Rezaei, M., Yazdani, M., Mogharabi-Manzari, M., Opportunities and Challenges in Biomedical Applications of Metal–Organic Frameworks, *J. Inorg. Organomet. Polym. Mater*. 31(12), 4443–4462 (2021). https://doi.org/10.1007/s10904-021-02118-7

Sanaei-Rad, S., Ghasemzadeh, M. A., Razavian, S. M. H., Synthesis of a novel ternary ZIF-8/GO/MgFe2O4 nanocomposite and its application in drug delivery, *Sci. Rep.* 11(1), 18734 (2021). https://doi.org/10.1038/s41598-021-98133-2

Shahsavari, M., Jahani, P. M., Sheikhshoaie, I., Tajik, S., Afshar, A. A., Askari, M. B., Salarizadeh, P., Di Bartolomeo, A., Beitollahi, H., Green Synthesis of Zeolitic Imidazolate Frameworks: A Review of Their Characterization and Industrial and Medical Applications, *Materials (Basel).* 15(2), 1–27 (2022). https://doi.org/10.3390/ma15020447

Subhadarshini, A., Samal, S. K., Pattnaik, A., Nanda, B., Facile fabrication of plasmonic Ag/ZIF-8: an efficient catalyst for investigation of antibacterial, haemolytic and photocatalytic degradation of antibiotics, *RSC Adv*. 13(45), 31756–31771 (2023). https://doi.org/10.1039/D3RA04851A

Thakur, S., Bharti, S., The synergy of nanoparticles and metal-organic frameworks in antimicrobial applications: A critical review, *J. Environ. Chem. Eng*. 11(6), 111458 (2023). https://doi.org/10.1016/j.jece.2023.111458

Yan, L., Gopal, A., Kashif, S., Hazelton, P., Lan, M., Zhang, W., Chen, X., Metal organic frameworks for antibacterial applications, *Chem. Eng. J.* 435(P2), 134975 (2022). https://doi.org/10.1016/j.cej.2022.134975

Yuan, J., Li, Q., Shen, J., Huang, K., Liu, G., Zhao, J., Duan, J., Jin, W., Hydrophobic-functionalized ZIF-8 nanoparticles incorporated PDMS membranes for high-selective separation of propane/nitrogen, *Asia-Pacific J. Chem. Eng.* 12(1), 110–120 (2017). https://doi.org/10.1002/apj.2058